

## Multiplexed Detection of Waterborne Pathogens in Circular Microfluidics

Shailaja Agrawal · Amit Morarka · Dhananjay Bodas ·  
K. M. Paknikar

Received: 30 October 2011 / Accepted: 1 February 2012 /  
Published online: 26 February 2012  
© Springer Science+Business Media, LLC 2012

**Abstract** Microfluidic lab-on-a-chip presents an ideal solution for bacterial sensing and identification due to its advantages like large surface-to-volume ratio, requirement of low sample volume and multiplexing possibility. The present work deals with the development of an immunosensor chip using circular microchannels fabricated directly with microdimensional copper wire and permanent magnet for capture of  $\text{Fe}_3\text{O}_4$  magnetic nanoparticle (MNP) conjugate. The MNP facilitate capture of the antigen in a confined space and hence, enhanced fluorescence signal for detection. The multiplexed microfluidic chip permits visual detection and quantification of waterborne pathogens viz. *Escherichia coli* and *Salmonella typhimurium* simultaneously. CdTe quantum dots (QDs) with different emission wavelengths were conjugated with anti-*E. coli* and anti-*S. typhimurium* antibodies for concurrent fluorescence detection. The present technique provides an inexpensive yet powerful tool to image and quantify pathogens at low numbers with passage of large sample volumes.

**Keywords** 3D circular microchannels · *E. coli* · *S. typhimurium* · QDs

### Introduction

Waterborne diseases are a key threat to developing as well as developed countries [1, 2] affecting thousands of lives [3–6]. According to the Centers for Disease Control and Prevention (CDC), annually, millions of people in the United States fall ill because of the waterborne pathogens [7]. Thus, life-threatening illnesses caused by bacteria continue to be a cause of concern all over the world.

Members of the family Enterobacteriaceae, in general, and *Escherichia coli* and *Salmonella typhimurium*, in particular, are the most common causative agents of food and waterborne diseases. These organisms cause gastrointestinal discomforts such as nausea,

---

**Electronic supplementary material** The online version of this article (doi:10.1007/s12010-012-9597-8) contains supplementary material, which is available to authorized users.

S. Agrawal · A. Morarka · D. Bodas · K. M. Paknikar (✉)  
Centre for Nanobioscience, Agharkar Research Institute, G.G. Agarkar Road, Pune 411 004, India  
e-mail: kpaknikar@gmail.com

D. Bodas  
e-mail: dhananjay.bodas@gmail.com

vomiting and diarrhoea, which could extend to life-threatening renal and hepatic complications in severe conditions [8, 9]. Enteric diseases could have tremendous impact at the socio-economic and public health levels; hence, timely detection of pathogens is essential. Conventional culture-based methods of pathogen detection are both time-consuming and cumbersome. Immunoassays, molecular methods based on DNA probes and polymerase chain reaction (PCR) based assays are not only rapid, sensitive and specific, but are mostly designed for detection of single species of pathogen [10]. Array-based immunosensors can achieve multiplexed detection using fluorescent dye-tagged antibodies. However, their practical utility suffers from inherent limitations such as photobleaching, narrow emission spectra and broad excitation spectra, making quantitative measurements of different species difficult. On the other hand, semiconductor quantum dots (QDs) have excellent photo-physical properties, like broad emission spectra and narrow excitation spectra. Further, QDs with different sizes can be excited with a single wavelength of light and give many characteristic narrow emission peaks simultaneously, making them suitable labels for multiplexing. A variety of applications describing successful use of QDs as labels in cellular imaging, bacterial detection etc. has been reported [11–14].

Besides use of appropriate labels, another important parameter influencing specific detection of bacteria is their number in the sample. For this purpose, conventional culture-based methods rely on bacterial isolation from test sample and their concentration or enrichment in culture media. Such procedures are reliable but laborious, time consuming (typically taking 18–24 h) and consume considerable quantities of media and reagents. Antibody-coated magnetic nanoparticle (MNP)-based immunomagnetic separation of bacteria is technically simple, rapid and specific for separation of target bacterial species directly from the sample without any preprocessing [15]. This rather well-established method, however, has rarely been used in a microfluidic format for detection of waterborne pathogens. Detection of foodborne pathogens using microfluidics such as optical biosensor, magnetoresistive immunosensors, electrochemical biosensor, waveguide sensor etc. has been, however, reported [16–24].

Considering the need for rapid, reliable, small and portable immunosensors which can be used for detecting multiple pathogenic organisms from water samples simultaneously, development of integrated microfluidic-based immunosensors is highly desirable. In this paper, we demonstrate on-chip, one-step multiplexing of bacteria by detecting *E. coli* and *S. typhimurium* on poly-(dimethoxy siloxane) (PDMS)-based platform. Microfluidic chip used for multiplexed detection consisted of two microchannels (500  $\mu\text{m}$ ) embedded with three permanent magnets each. In the capture zone, immunomagnetic separation of target bacteria (*E. coli* and *S. typhimurium*) in two different microchannels is achieved. Detection was done in the detection zone where captured bacteria could be visually identified by labelling with antibody-conjugated QDs (having distinct emissions, viz. 550 nm and 605 nm) using a fluorescence microscope.

## Materials and Methods

### Fabrication of Microfluidic Chip

Microfluidic chip with microchannels and permanent magnet for multiplexing was fabricated in PDMS by direct method [25, 26]. Metal wire (diameter 500  $\mu\text{m}$ ) was clamped on the device which was used as a mould. Three permanent magnets (diameter 2 mm) were embedded at a distance of 1.5 cm in the mould. Liquid PDMS was mixed in the ratio 10:1

(base:curing agent), degassed in vacuum desiccators for 20 min, poured on the mould and cured at 65 °C for 180 min. Cured PDMS was de-moulded from the device, and wires were drawn out by dipping the chip in ethanol while applying gentle force. Channels with one inlet and one outlet were used for the quantitative detection of individual bacterial species, while channels with single inlet and two outlets embedded with six magnets were used for multiplexed detection of different bacteria. The microfluidic chip was activated in oxygen plasma (Emitech: Model K-1050X) at RF power of 60 W for 1 min and coated with bovine serum albumin (BSA) (3% in phosphate-buffered saline (PBS)) to minimise non-specific interaction of antigen to the wall of capillary.

#### Synthesis of Quantum Dots (QDs)

Cadmium chloride ( $\text{CdCl}_2$ ), tellurium powder, thioglycolic acid (TGA, 98%), and sodium borohydrate ( $\text{NaBH}_4$ , 98%) were obtained from SRL Chemicals, India and used as received. All chemicals used were of analytical grade. CdTe QDs were synthesised by previously reported protocol [25]. Briefly, 0.0319 g of Te metal powder was mixed with 0.0289 g of  $\text{NaBH}_4$  in a round bottom flask and 1 mL  $\text{N}_2$ -saturated water was added with the help of a syringe. Throughout the reaction, inert atmosphere was maintained. The reaction was performed at room temperature with sonication till black Te powder changes to pink-coloured sodium hydrogen tellurite complex ( $\text{NaHTe}$ ). TGA-coated CdTe QDs were synthesised using  $\text{CdCl}_2$  and  $\text{NaHTe}$  as precursor. Freshly prepared  $\text{NaHTe}$  was added to 100 mL of  $\text{N}_2$ -saturated water containing  $\text{CdCl}_2$  and TGA (molar ratio 1:2.5). The pH of solution was adjusted to 11 with 1 M NaOH prior to the reaction. The mixture was refluxed at 100°C for 2 and 12 h to get different sizes of QDs with emission at 550 nm (green) and 605 nm (red), respectively.

#### Synthesis of Antibody Magnetic Nanoparticle (MNP) Conjugates

$\text{Fe}_3\text{O}_4$  MNPs (size <50 nm) purchased from Sigma-Aldrich were conjugated with polyclonal anti-*E. coli* antibody and anti-*S. typhimurium* antibody separately. Freshly prepared 0.4 M 1-ethyl-3-(3-dimethylaminopropyl) carbodiimide hydrochloride (EDC) in PBS (pH7.4) was mixed with MNPs at 1:1 ratio. After 15 min of incubation on rocker, the mixture of MNPs with EDC was washed, and antibody (1 mg/mL) was added in equal volume. Mixture was incubated at 4°C for 12 h with gentle shaking.

#### Synthesis of Antibody-QD Conjugates

TGA-capped QDs were conjugated with anti-bacterial antibody using EDC/*N*-hydroxysuccinimide (NHS) coupler [27]. Five molar solution of QDs was mixed with 5 mM NHS, 0.05 M EDC followed by the addition of respective antibody (1 mg/mL), and subsequently, this solution was incubated at room temperature for 2 h and then stored at 4°C. QD with green fluorescence were conjugated with anti-*E. coli* antibody and those with red fluorescence were tagged with anti-*S. typhimurium* antibody.

#### On-chip Immunoassay for Determining the Number of the Cells (*E. coli* and *S. typhimurium*)

Bacterial cells (*E. coli* ATCC 117 and *S. typhimurium*) were cultured in Luria–Bertini broth (LB broth) at 37°C for 16 h. Cells were centrifuged at 6,000 rpm for 10 min and washed with PBS (pH 7.4). The absorbance was monitored at 600 nm. Five tenfold dilution of culture

(0.1 OD $\approx$ 10<sup>8</sup> cells/mL) were prepared in PBS approximately ranging from 10<sup>7</sup> to 10<sup>3</sup> cfu/mL. *E. coli* and *S. typhimurium* culture (10<sup>5</sup> cfu/mL) were used to demonstrate the multiplexing.

### On-chip Multiplexed Detection of Bacteria

Antibody-conjugated MNPs were captured on two different magnets of pre-capture zone. To avoid the mixing of antibody-conjugated MNPs, separate outlets were used to inject MNP anti-*E. coli* Ab and MNP anti-*Salmonella* antibody. Teflon tube at the inlet was preloaded with 20  $\mu$ L of test antigen (*E. coli* and *S. typhimurium*, 1:1 ratio), 20  $\mu$ L of Ab–QD solution (Ab–QD550 and Ab–QD605), and buffer. Reagents were separated by air plug in the inlet tube. The whole assembly was connected to syringe pump (Harvard instruments) and a constant flow rate 10  $\mu$ L/min was maintained. Removal of permanent magnets from pre-capture zone causes the movement of MNP–Ab conjugate towards capture zone along with the flow of antigen. Channels were washed with PBS to remove the non-specific components of test sample. In the next step, magnets from the capture zone were removed and QD–Ab solution was allowed to flow. Finally, QD–Ab bound antigen–MNP complex was captured over the magnet of detection zone which was imaged using upright fluorescent microscope equipped with CCD (Nikon H600L, Japan) and analysed using Image Pro Plus (version 6.0) software supplied with the camera. The surface of the channels was blocked with BSA (3% BSA in PBS, pH 7.4) prior to addition of MNP–Ab conjugate.

## Results and Discussion

A representative figure of the arrangement of magnet and metal wire (copper) in microfluidic device used is shown in Fig. 1. A similar setup was used for embedding three magnets beneath the metal wire. Also, two metal wires forming one inlet and two outlets (used for multiplexing) with six magnets embedded was formed using a similar arrangement. This device was used for clamping microwires and moulding PDMS for fabrication of microchannels with embedded permanent magnet. The wire was drawn out by applying a gentle force leading to formation of a circular microchannel in PDMS. A photograph of complete microfluidic chip with the entire zone is shown in Fig. 2. Chip used for detection of different concentrations of antigens with multiplexing is shown in Fig. 3. Schematic of immunoassay

**Fig. 1** Schematic of device used for clamping microwires and moulding PDMS

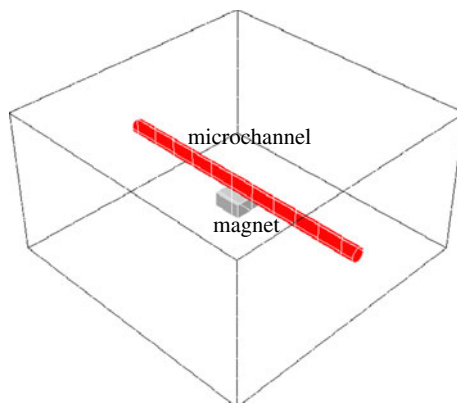
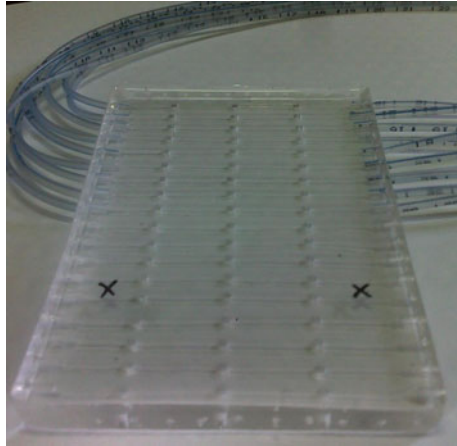


**Fig. 2** Chip used for detection of different cell densities of *E. coli* and *S. typhimurium*



and reusability of channels is represented in Fig. 4. Three permanent magnets compartmentalised the chip into pre-capture zone, capture zone, and detection zone. With the permanent magnet in pre-capture zone, chip was loaded with MNPs–Ab conjugate through separate channels which help to capture specific antigen in a specific channel. The flow rate was adjusted such that the target antigen binds with MNPs and the non-specific component washed off. In the next step, captured antigen was detected with the help of QDs–Ab complex. Removal of external magnet causes movement of MNPs, antigen and QDs which helps to regenerate channels for additional assay.

For the detection of multiple waterborne organisms in a single chip, two types of QDs were synthesised. It is important to note that different sizes of the CdTe QDs give different fluorescence colours which can be controlled by varying the refluxing time. In our work, we synthesised QDs with green and red fluorescences. Typical photoluminescence (PL) spectra of TGA-coated CdTe QDs with two different refluxing times with incubation time 2 and 12 h showed emission at 550 nm (green) and 605 nm (red), respectively. With the increase of refluxing time, the size of the nanocrystals increase, and as a result of quantum confinement effect, the absorption maximum of  $1\text{ s}^{-1}$  electronic transition shifts to a longer emission wavelength. In addition to this property of QDs, PL spectra also shows a narrow and symmetric band which verifies narrow size distribution.

**Fig. 3** Chip used for multiplexing of waterborne bacteria



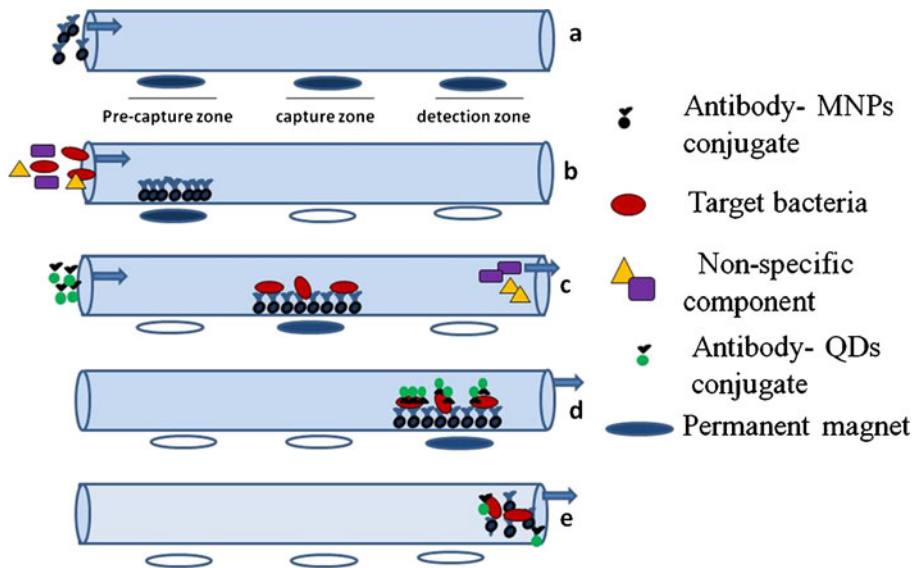


**Fig. 4** Schematic representation of immunoassay: **a** entrapment of antibody-conjugated MNP with the help of embedded permanent magnet (field strength 0.3 T); **b** and **c** capture of target antigen; **d** detection of captured antigen with quantum dot antibody conjugate; and **e** regeneration of channels

The conjugation of TGA-coated QDs with antibody was confirmed by Fourier transform infrared (FTIR) spectra.  $-\text{COOH}$  group present on the surface of QDs interacts with antibody in the presence of EDC and NHS to form linkage. Peak difference at  $1,197\text{ cm}^{-1}$  demonstrates the conjugation. Likewise, confirmation of the conjugation of  $\text{Fe}_3\text{O}_4$  NPs with antibody is proved as a peak at  $1,128\text{ cm}^{-1}$  corresponding to ester linkage could be clearly observed. Additional peaks at  $905$  and  $705\text{ cm}^{-1}$  corresponds to the phosphate group present in PBS observed only in the spectra of antibody conjugates.

Immunoassay was performed for optimisation of capture of target antigen, *E. coli* and *S. typhimurium* separately over the working range of  $10^3$ – $10^7$  cfu/mL. Optical images of detection zones precisely above the magnet for *E. coli* and *S. typhimurium* were shown in Figs. 5 and 6, respectively. High contrast images processed using a freeware, ImageJ, show increase in the number of bacteria from  $10^3$  to  $10^7$  cfu/mL. The  $\text{Fe}_3\text{O}_4$  NPs capture the inflow antigen from a test sample in a confined space and enhanced fluorescence signal was obtained from QDs. The fluorescent signal was recorded as absolute intensity from the channel where maximum MNPs are trapped and plotted against the cell concentration as

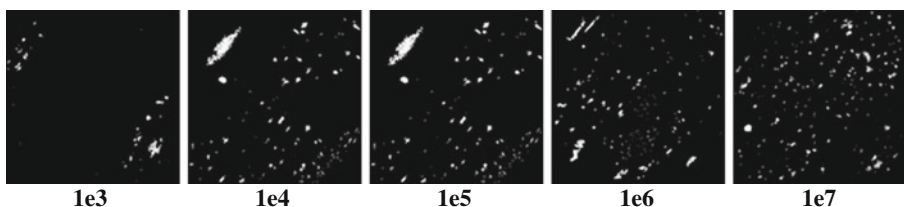


**Fig. 5** High contrast fluorescence images of different *E. coli* densities captured by magnet at detection zone

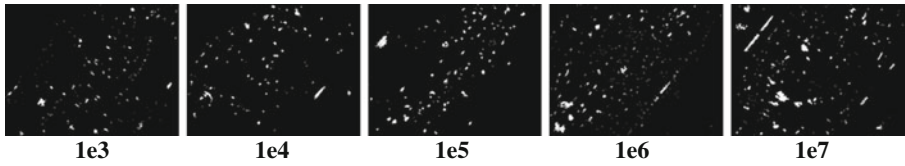
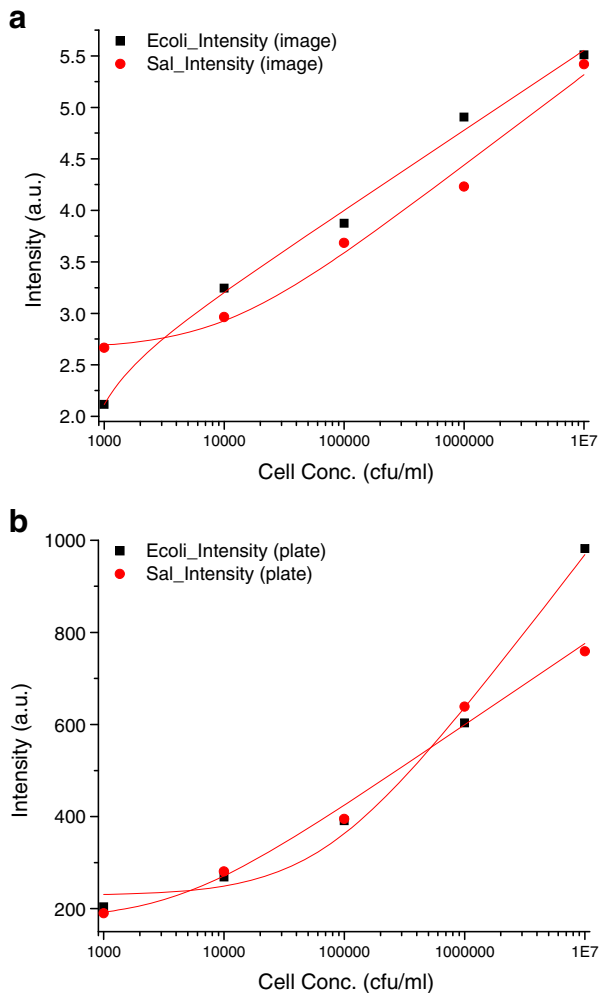


**Fig. 6** High contrast fluorescence images of different *S. typhimurium* densities captured by magnet in detection zone

shown in Fig. 7a. The images were processed using ImageJ to find the number of cells. The images were processed by first converting an image to greyscale and then determining intensity maxima points. The maxima points were obtained from the points where QDs fluoresce. An average of the maxima points were considered as the total intensity

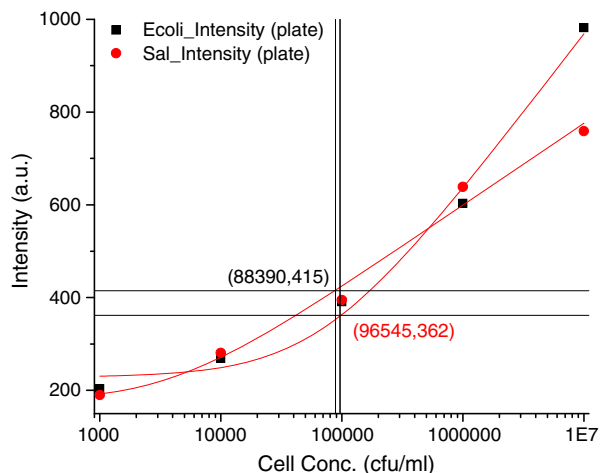
**Fig. 7** Graph showing fluorescence intensity variation with cell density for two different bacteria (*E. coli* and *S. typhimurium*): **a** data captured from images and **b** from fluorimeter



corresponding to the QDs and hence, the cell density. From Fig. 7a, it could be seen that the fluorescence intensity varies linearly with the number of *E. coli* and *S. typhimurium* which is in accordance with a previously published report [27]. The reason for small variation in the linearity is because of the use of polyclonal antibody for capture as detection. This opens up a new possibility of a very low cost quantification technique which could be used as a preliminary screening method. To confirm the results obtained with image acquisition and processing, the sample was collected after the capture and processed in a fluorimeter to get an accurate reading for the fluorescence. The specificity of the assay was confirmed by measuring the fluorescent intensity. For fluorimetric estimation, samples were eluted from the detection zone, suspended in 50  $\mu\text{L}$  of PBS and fluorescence was measured using a Synergy II plate reader fluorimeter (BioTek). Samples were processed in a 96-well opaque bottom fluorescence plate (Corning) and excited at 480 nm from the top. This arrangement could help to minimise the interference of MNPs in fluorescence measurement. The fluorescence intensity was recorded via a filter at emission wavelengths of 528 and 590 nm. This reading was directly proportional to the cell density and was plotted against fluorescence intensity (Fig. 7b). The trend observed in Fig. 7a and b depicts a linear increase in fluorescence intensity with cell density. The curve fitting carried out for *E. coli* and *S. typhimurium* gives  $R^2$  values of 0.993 and 0.985, respectively, which proves statistical linearity of the data.

The capability of microfluidic chip for multiplexing was demonstrated with some modification in the basic design of the chip as was used for concurrent detection of *E. coli* and *S. typhimurium*. A fluorescence image was captured just above the magnet of the detection zone following the protocol and the sample processed using a fluorimeter as described earlier. Figure 8 shows a graph of fluorescence intensity versus cell density for the readings obtained from a fluorimeter. The intercept on the  $y$ -axis shows the reading of *E. coli* and *S. typhimurium* when simultaneously detected using a ‘single inlet–multi outlet’ chip (see Fig. 3). Both organisms were flown through the microchannel (cell density  $10^5$  cfu/mL) and as the intercept on the  $x$ -axis indicates, the detected densities of *S. typhimurium* and *E. coli* were  $8.8 \times 10^5$  cfu/mL and  $9.6 \times 10^5$  cfu/mL, respectively. These results prove the accuracy and specificity of detection.

**Fig. 8** Graph showing comparative estimation of cells (*E. coli* and *S. typhimurium*) detected by multiplexing





## Conclusion

We have demonstrated an effective method of MNPs and QD-based immunoassay for the separation and concentration of two bacterial species using multiplexed microfluidic technology. Microchannels used in the current study are fabricated by a simple one-step method which is straightforward, easy, fast, and repeatable. Different cell densities of *E. coli* and *S. typhimurium* ranging from  $10^3$  to  $10^7$  cfu/mL were detected using the MNP pre-concentration technique in a microchannel. It is possible to detect both *E. coli* and *S. typhimurium* in 1:1 concentration from a single source using a microfluidic-based multiplexing technique and two types of QDs (green and red). This method is rapid, sensitive, reliable, less reagent consuming, and cost effective. The study opens up many possibilities of use of microchannels for bacterial detection and is likely to lead to development of inexpensive methods for screening a variety of clinical, water, food, and environmental samples for multiple organisms.

**Acknowledgement** S. Agrawal is grateful to the Council of Scientific and Industrial Research (CSIR), India for the award of a Junior Research Fellowship.

## References

1. Antony, B., Dias, M., & Shetty, A. K. (2009). *Indian Journal of Medical Microbiology*, 27(3), 257–258.
2. Chugh, T. D. (2008). *J Biosciences*, 33(4), 549–55.
3. Gandhi, N. R., Nunn, P., Dheda, K., Schaaf, H. S., Zignol, M., van Soolingen, D., Jensen, P., & Bayona, J. (2010). *Lancet*, 22, 1830–43.
4. Abhirosh, C., Sherin, V., Thomas, A. P., Hatha, A. A. M., & Mazumder, A. (2011). *Public health*, 125, 377–379.
5. Aycicek, H., Aydogan, H., Kuc, A., Ukkaraaslan, Baysallar, M., & Basustaoglu, A. C. (2004). *Food Control*, 15, 253–254.
6. Aarestrup, F. M., Hendriksen, R. S., Lockett, J., Gay, K., Teates, K., McDermott, P. F., White, D. G., & Hasman, H. (2007). *Emerg. Infect. Dis.*, 13(5), 726–731.
7. Scallan, E., Hoekstra, R. M., Angulo, F. J., Tauxe, R. V., Widdowson, M.-A., et al. (2011). *Emerg. Infect. Dis.*, 17, 1.
8. DuPon, H. L., Hornick, R. B., Snyder, M. J., Libonati, J. P., Sheahan, D. G., Eugene, M. B., LaBrec, H., & Kalas, J. P. (1979). *N Engl J Med.*, 28, 1–9.
9. Santos, R. L., Tsolis, R. M., Bäuml, A. J., & Adams, L. G. (2003). *Braz J Med Biol*, 36, 1.
10. Mandal, P. K., Biswas, A. K., Choi, K., & Pal, U. K. (2011). *American Journal of food Technology*, 6(2), 87–102.
11. Chan, W. C., Maxwell, D. J., Gao, X., Bailey, R. E., Han, M., & Nie, S. (2002). *Current Opinion in Biotechnology*, 13, 40–46.
12. Wu, X., Liu, H., Liu, J., Haley, K. N., Treadway, J. A., Larson, J. P., Ge, N., Peale, F., and Bruchez M. P. (2003) *Nature biotechnology*, 21.
13. Yang, L., Ren, X., Meng, X., Li, H., & Tang, F. (2011). *Biosensors and Bioelectronics*, 15, 3488–3493.
14. Aldeek, F., Mustin, C., & Balan, L. (2011). Thibault Roques-Carmes, Marie-Pierre Fontaine-Aupart, Schneider, R. *Biomaterials*, 32, 5459–5470.
15. Chakraborty, R., Hazen, T. C., Joyner, D. C., Küsel, K., Singer, M. E., Sitte, J., & Torok, T. (2011). *Journal of Microbiological Methods*, 86, 204–209.
16. Fedio, W. M., Jinneman, K. C., Yoshitomi, K. J., Zapata, R., Wendakoon, C. N., Browning, P., & Weagant, S. D. (2011). *International Journal of Food Microbiology*, 148, 87–92.
17. Li, Y., & Su, X. L. (2006). *J. Rapid Methods Autom. Microbiol*, 14, 96–109.
18. Mujika, M., Arana, S., Castano, E., Tijero, M., Vilares, R., & Ruano-Lopez, J. M. (2009). *Biosens Bioelectron*, 24, 1253–1258.
19. Zourob, M., Mohr, S., Brown, B. J. T., Fielden, P. R., McDonnell, M. B., & Goddard, N. J. (2005). *Biosens Bioelectron*, 21, 293–302.

20. Boehm, D. A., Gottlieb, P. A., & Hua, S. Z. (2007). *Sens. Actuat. B*, 126, 508–514.
21. Ivnitski, D., Abdel-Hamid, I., Atanasov, P., Wilkins, E., & Stricher, S. (2000). *Electroanalysis*, 12, 371–325.
22. Gehring, A. G., & Shu-I, Tu. (2011). *Annu Rev Anal Chem*, 4, 151–72.
23. Yakovleva, J., Davidsson, R., Lobanova, R., Bengtsson, M., Eremin, S., Laurell, T., & Emneus, J. (2002). *Anal Chem*, 74, 2994–3004.
24. Ertl, P., Wagner, M., Corton, E., & Mikkelsen, S. R. (2003). *Biosens Bioelectron*, 18, 907–916.
25. Morarka, A., Agrawal, S., Kale, S., Kale, A., Ogale, S., Paknikar, K., & Bodas, D. (2011). *Biosens Bioelectronics*, 26, 3050–3053.
26. Agrawal S, Morarka A, Paknikar K, Bodas D (2011) Microelectronic Engineering. In Press.
27. Zhu P, Shelton DR, Li S, Adams D, Karns JS, Amstutz P, Tang C-M (2010) Biosensors and Bioelectronics doi:10.1016/j.bios.2011.09.029